Penerbit Akademia Baru

Journal of Advanced Research Design

Journal homepage:
https://akademiabaru.com/submit/index.php/ard
ISSN: 2289-7984

Design and Analysis of Vortex Induced Vibration Suppression Device

Syamsul Azry Md Esa[1], Nor Azwadi Che Sidik[1,2,*]

[1] Faculty of Mechanical Engineering, Universiti Teknologi Malaysia, 81310 Skudai, Johor, Malaysia
[2] Malaysia – Japan International Institute of Technology (MJIIT), University Teknologi Malaysia Kuala Lumpur, 54100 Kuala Lumpur, Malaysia

ARTICLE INFO

Article history:
Received 20 May 2021
Received in revised form 17 September 2021
Accepted 4 October 2021
Available online 15 October 2021

Keywords:
Vibration suppression; hydrodynamic; analysis of vortex

ABSTRACT

The purpose of this study was to investigate the effectiveness of fairing as a device to suppress vortex-induced vibration (VIV) of a cylindrical structure which is commonly used as a riser and conductor in the oil and gas industry. This phenomenon is caused by the interaction between a structure and shed vortices which can result in large amplitude vibrations of the structure that may lead to severe damage over time. Repairs to these systems are costly and time-consuming, hence significant effort has been expended to develop a means of eliminating the need of repairs from vibrations. Passive methods of altering the flow behaviour around the cylindrical structure to mitigate the hydrodynamic forces that cause VIV were considered. As a result, structural enhancements to a cylinder which use fairing was attempted to accomplish this goal. This study was performed through numerical analysis by investigating the drag coefficient and lift coefficient of bare cylinder when subjected to a typical maximum fluid flow speed range from metocean data for Malaysia region, and comparing it with the data produced when cylinder is applied with fairing of different chord lengths. These marine structures could sustain longer during its service life and hence could reduce the maintenance cost for the operator as the fatigue life increases due to the application of fairing. Validation of numerical model against the data from literature was also performed to ensure that the outcomes of this analysis can be used for other related future study. This numerical analysis was conducted using commercially available computational fluid dynamics (CFD) software ANSYS Fluent version 16. Navier-Stokes equations were solved in the simulation to obtain the results of the study.

1. Introduction

Petroleum industry is one of the primary industries in the world. Structural reliability is among the important factor for offshore design structure. A lot of money has been paid by the oil and gas industry player to perform maintenance and reparation of the riser system which mainly consist of cylindrical structure system so called risers and conductors.

Vortex-induced vibration (VIV) become one of most important design consideration. Insufficient understanding of VIV causes significant increase in cost due to large safety factor applied. Test data are also not extensively available in public domain due to proprietary nature in industry. Figure 1

* *Corresponding author.*
E-mail address: azwadi@semarakilmu.com.my

shows an offshore platform with the wells for oil and gas, as well as the risers consist of cylindrical form structures which are commonly used in the oil and gas industry.

Fig. 1. Cylindrical structures on an offshore platform

Riser or conductor can be either rigid or flexible connection between a platform and a wellhead on sea bed. Figure 2 shows the typical location and configuration of the riser and conductor.

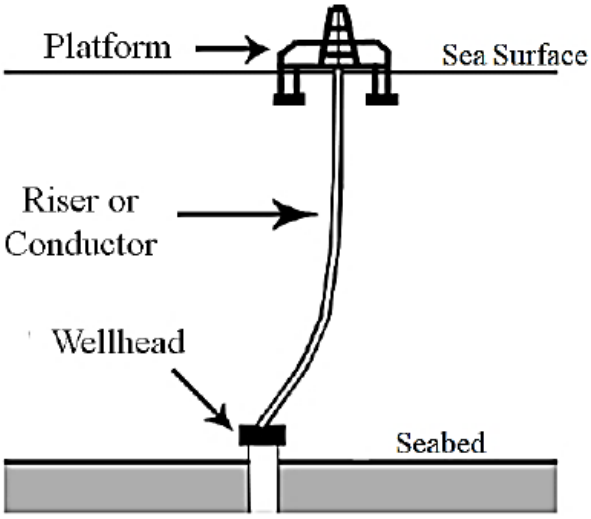

Fig. 2. Sketch for riser/conductor system principle

Cylindrical structures such as marine risers are exposed to a so-called VIV phenomenon. Conductor pipes such as rigid risers will experience extensive oscillations or vibrations, which can lead to high frequency cyclic stresses, resulting in high rates of fatigue damage or premature failure. This detrimental effect is severe for drilling risers, and even more so for production risers where service life of more than 25 years is often required. Thus, this study aimed to reduce the effect of VIV phenomenon and hence reducing the risk of damaging the cylindrical structure such as conductor pipe used in the oil and gas industry.

2. Literature Review

VIV of structures is of practical interest to many fields of engineering. Cylindrical structures such as marine risers in deep water applications are prone to this phenomenon, which is due to the regular shedding of vortices from the riser when exposed to unsteady current flow. The primary purposes of this structure are not to gain lift or minimize drag as it is with aircraft components, but rather to bear loads, contain flow or provide heat transfer [1]. Association of VIV in the interaction between fluids and riser is subjected to extensive researches in both industries and academic field over the past few decades due to high demand in exploring hydrocarbon resources.

Karman vortex shedding occurs due to the flow separation around any structure [2]. When the vortex shedding frequencies are synchronized with natural frequencies of a riser along a considerable length, the system is said to be in a "lock in" range. As a result, the conductor pipe will experience extensive oscillations or vibrations, which can lead to high frequency cyclic stresses, resulting in unacceptable high rates of fatigue damage or premature failure to the structure [3]. This detrimental effect is severe for drilling risers, and even more so for production risers where normally the service of more than 25 years is required. Generally, deep water risers are most susceptible to complex VIV response because current flow intensity can be different along the different depths in deep water areas.

There are two possible motions of a cylinder structure such as riser when subject to current flow, namely the in-line motion and transverse or cross-flow motion. Figure 3 shows the direction of the possible motions for a cylinder when subjected to a current flow.

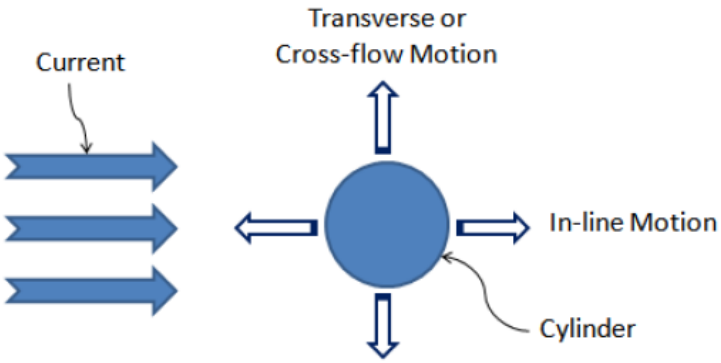

Fig. 3. Motions of a cylinder when subjected to current flow

Studies on the vibration of circular cylinders in oscillating flow began with structures exposed to open ocean waves in marine engineering applications. Morison *et al*., [4] proposed a modeling method where the force on the structure in oscillating flow is expressed as the summation of inertia and drag forces. A lot of researchers still use this method.

Rahman *et al*., [5] studied the unsteady flow passed a circular cylinder using a 2D finite volume method with different Reynolds number (Re). They found that, as Re becomes higher than 40 the flow reports a loss of symmetry in the wake. The studiy also reported the Strouhal number (St) was found to be 0.164 for Re=100. Vijaya *et al*., [6] investigated 2D unsteady flows of power-law fluids over a cylinder. The study concluded using a finite volume method as solver.

Mittal and Kumar [7] studied VIV on a pair of equal-size cylindrical cylinders with two sets of arrangement, inline and staggered. The fixed cylinders for the 2D simulation were simulated in a rectangular computational domain with a fixed Re = 1000. They concluded that for a circular cylinder, flow separation point changes with Re, so the wake was unsteadiness. They also concluded that the

oscillations of the cylinders result in an alternate mode of vortex shedding and where the vibration of cylinders is usually accompanied by an increase in drag.

Shao and Zhang [8] used the finite volume method to investigate two side-by-side cylindrical cylinders. The cylinders were simulated in a 23 times of the cylinder diameter computational domain with a constant inlet velocity of 7 m/s. They concluded that large eddy simulation (LES) was capable of reproducing complex subcritical turbulent wake behind a circular cylinder, but fine meshes and longer time were required for the flow around the circular cylinder.

Bourguet *et al*., [9] studied lock-in of the VIV on an in-line flow of a flexible cylindrical cylinder using direct numerical simulation (DNS) of the 3D incompressible Navier-Stokes equations. They concluded that the structural vibrations were mixtures of standing and traveling wave patterns. A frequency ratio of approximately 2 can be established between the excited frequencies in the in-line and cross-flow directions.

Pratish and Tiwari [10] investigated unsteady wakes behind two inline arrangement of square cylinders. 2D computational domain was used where the length and width of the channel were 16 and 6 times of the square width cylinders, respectively.

Chandrakant and Swapnil [11] analyzed vortex shedding behind a D shaped cylinder. 2D computational domain with 2 m length and 1.6 m, and quad meshing was used for the study. They also reported that the Strouhal number increased with the increase in Re and the number of vortices increases with Re.

Ali and Edris [12] analyzed the numerical simulation of unsteady flow with vortex shedding around circular cylinder. 2D flow of an incompressible fluid around a circular cylinder were simulated in both uniform stream flow and oscillated flows at Re = 300. The computational domain with length, 0.3 m and width, 0.2 m with water as the assumption liquid was used in the study.

Roshko [13] found out that vortex shedding was not observed at Re <$3.5x10^6$. Below the value of Re <$3.5x10^6$, no peak frequency occurred, but above this value there appeared a strong spectral peak, said to be well above the turbulence level.

Synchronization occurs when the cylinder natural frequency was near to the vortex shedding frequency, leading to lock-in and hence large amplitude vibrations. Lock-in occurs in both the cross-flow and in-line directions [1].

Karman vortex shedding arises due to flow separation around the structures [14]. It has been an important subject of study due to its direct relation to the excitation for frequency. The alternate shedding of vortices behind the structures lead to periodic pressure oscillations both in transverse as well as flow directions [15-17]. At this stage, the vortex shedding frequency is matched with the oscillation frequency of the cylinder structures. However, pressure oscillations occur at double the vortex shedding frequency in the flow direction. It is known also known that Strouhal number varies with Re, surface roughness and turbulence intensity [18-20].

A cylinder will be exposed not only to the periodical vortex shedding induced forces but also to broad band turbulence. The latter excitation becomes relatively more significant when the periodic shedding frequency is far from the structural frequency. Both turbulences propagated from upstream and turbulence play an important role.

3. Methodology

In general, CFD solution method consists of three main steps which are pre-processing, solver and post-processing. Schematic diagram for the process flow of this study is shown in Figure 4 below.

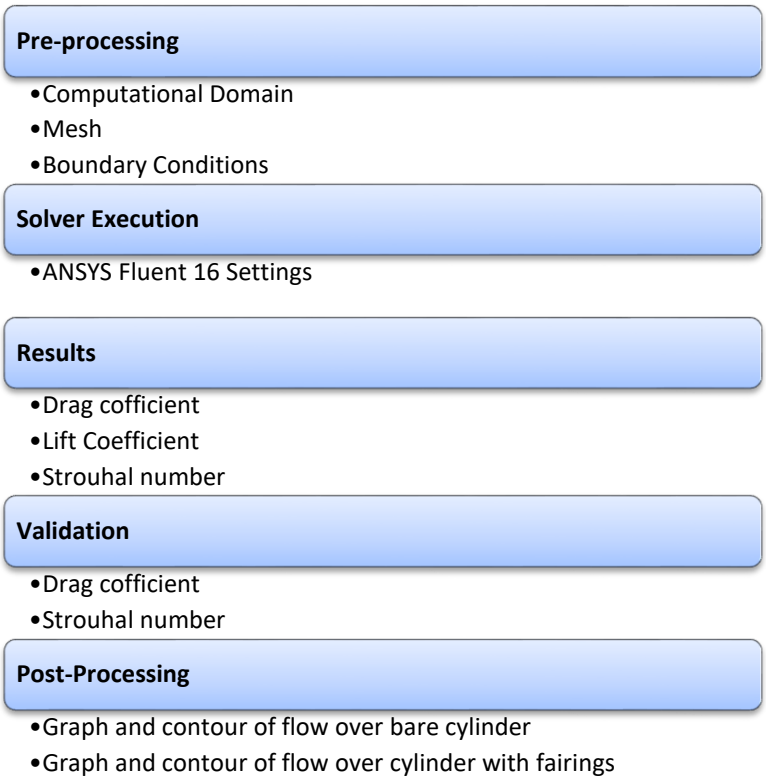

Fig. 4. Schematic diagram of CFD solution method

3.1 Relevance of Design Inputs

Cylinder with diameter of 0.5 m was chosen to be used in the study because it lies in one of the common range for riser and conductor in oil and gas industry. This size was neither too small nor too big for the application. Properties of water such as density and viscosity (kinematic and dynamic) were used instead of sea water because a lot of experimental data in laboratory used water. The results could be then compared more accurately with the experimental data from laboratory. In addition to that, the difference in terms of density and viscosity between water and sea water is relatively small.

Cylinder is subjected to a flow speed of 0.5 - 2.0 m/s with the incremental value of 0.5 m/s. These values were selected as these should cover the typical maximum current speeds of metocean data in Malaysia region for up to 100 years extreme storm condition. When performing back calculation with the other inputs data, the flow speeds used in the analysis represent the Re of between 10^5 and 10^6. This range Re is considered high and lies within the range of turbulent flow.

There were three configurations of cylinder used in this study namely bare cylinder, cylinder with chord length of 1.25D and cylinder with chord length of 1.5D. Lower value of chord length was not considered due to the space required when installing the bearing mechanism to allow the fairing to be weathervane in actual condition. On the other hand, higher values of chord length was not included due to practicality of fairing in the application, whereby longer fairing chord length contributed to greater weight as well as cost increase. Design inputs for this study are summarized in Table 1.

Table 1
Design inputs

Item	Detail	
Geometry	Size of bare cylinder	0.5 m
Fluid Properties (Water)	Density	998.2 kg/m^3
	Dynamic viscosity	1×10^{-3} kg/m^3
	Kinematic viscosity	1×10^{-6} m^2/s
Flow Speed	Four variations	0.5 m/s
		1.0 m/s
		1.5 m/s
		2.0 m/s
Corresponding Reynolds Number	Four variations	$2.49\text{E}+05$
		$4.98\text{E}+05$
		$7.46\text{E}+05$
		$9.95\text{E}+05$
Fairing Chord Length	Two variations	1.25D
		1.5D

3.2 Simulation Variables

The analysis was categorized into 3 main variables; Independent variable, dependent variable and controlled variable. The speed of fluid flow or the Re and the cylinder configurations were the independent variables in this study. Three different configurations of cylinder are shown in Figure 5.

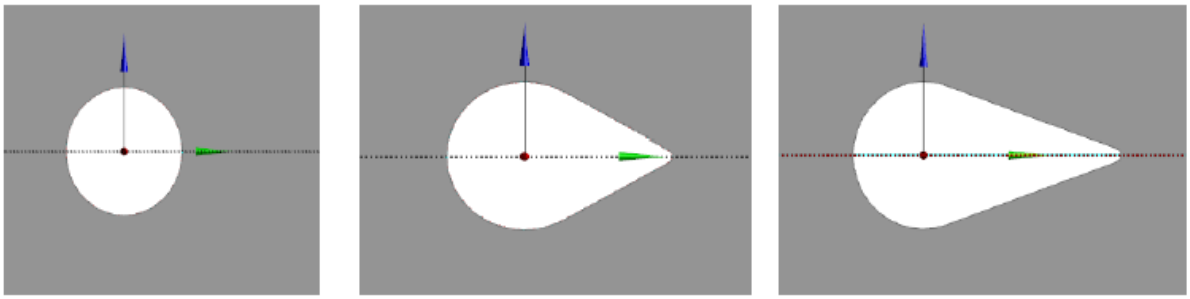

(a) (b) (c)

Fig. 5. Configurations of cylinder (a) Bare cylinder (b) F1.25D and (c) F1.5D

The dependent variables or the parameters that were extracted from the output of the analysis were drag coefficient (Cd), lift coefficient (Cl) and Strouhal number (St). Controlled variables or parameters that were constant throughout the simulation were fluid temperature, fluid density and fluid viscosity (kinematic and dynamic). Details of variables are summarized in Table 2.

Table 2
Details of variables

Items	Details
Independent Variables	Flow speeds / Reynolds number
	Fairing Chord Length
Dependent Variables	Drag coefficient, C_d
	Lift coefficient, C_l
	Strouhal Number
Controlled Variable	Fluid Temperature
	Fluid Density
	Fluid Viscosity

3.3 Test Matrix

The analyses were conducted with 3 sets of data. The set were differentiated with the type of cylinder configurations used. Each set consists of four load cases which were varied in terms of the fluid flowing speed. Strouhal number (St), drag coefficient (Cd) and lift coefficient (Cl) were extracted as the output results. The test matrix is summarized as in Table 3.

Table 3
Test matrix

Item	Load Case	Input Variables		Output Variables			
		U	Re	St	Cd	Cl	Cl/Cd Ratio
		m/s	-	-	-	-	-
Bare Cylinder	1	0.50	$2.49E+05$	-	-	-	-
	2	1.00	$4.98E+05$	-	-	-	-
	3	1.50	$7.46E+05$	-	-	-	-
	4	2.00	$9.95E+05$	-	-	-	-
Cylinder with Fairing 1.25D	1	0.50	$2.49E+05$	-	-	-	-
	2	1.00	$4.98E+05$	-	-	-	-
	3	1.50	$7.46E+05$	-	-	-	-
	4	2.00	$9.95E+05$	-	-	-	-
Cylinder with Fairing 1.5D	1	0.50	$2.49E+05$	-	-	-	-
	2	1.00	$4.98E+05$	-	-	-	-
	3	1.50	$7.46E+05$	-	-	-	-
	4	2.00	$9.95E+05$	-	-	-	-

Note: - = Results yet to be known

3.4 Parameters for Model Validation

In order to create a simulation baseline model that is then used throughout the different cylinder configurations, few preliminary simulations for flow over bare cylinder were generally performed using default parameters in the Ansys Fluent software. These miscellaneous parameters are available in the software were then fine-tuned once at a time so that two parameters such as the drag coefficient (Cd), as well as Strouhal number (St), that are used for validation are matched as close as possible.

The first validation for the baseline model was done using the comparison of the drag coefficient (Cd) between the results obtained from preliminary simulations and the established plot of drag coefficient (Cd) versus Re for a smooth cylinder. The data of the plot showing this relationship between drag coefficient and Re was produced by H Schlichting and is available in many fluid mechanics literatures. The plot is shown in Figure 6.

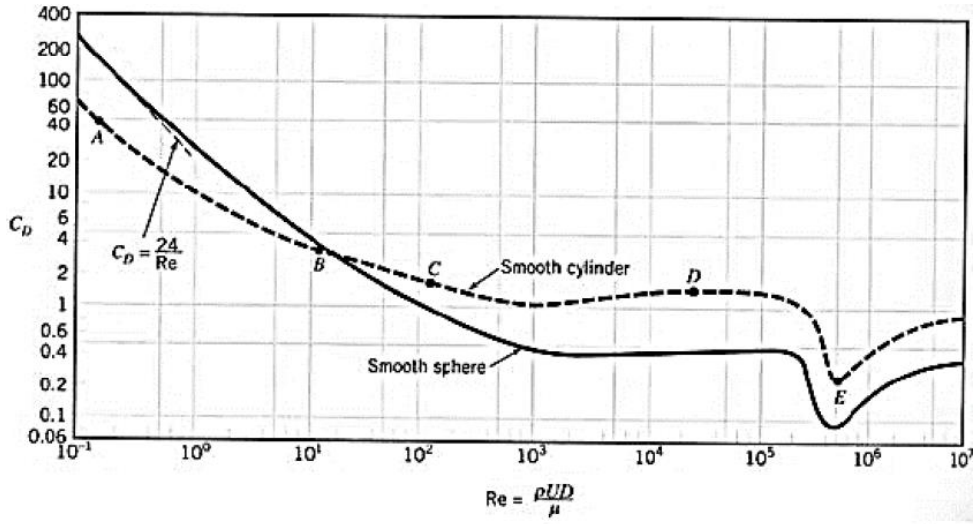

Fig. 6. Plot of drag coefficient vs Reynolds number

Re range of interest for this study lies in the 105 - 106 regions which correspond to flow speed of 0.5 - 2.0 m/s flow over a 0.5 m diameter of cylinder. The drag coefficient (Cd) in the region of interest as mentioned above should be in the range of 0.2 and 1.2. Should the drag coefficient (Cd) obtained was not within the range of these expected values, other parameters available in the Ansys Fluent software are required to be fine-tuned. Example of parameters than can be fine-tuned includes the mesh type and size, type of solver, intensity of turbulence and surface roughness. These steps are continued to take place until the drag coefficient (Cd) obtained, were within the expected range.

The second validation for the baseline model was done using the comparison of the Strouhal number (St) between the results obtained from preliminary simulations and the established plot of Strouhal number (St) *vs* Re for a smooth cylinder. The data of the plot showing this relationship between Strouhal number and Re is depicted in Figure 7.

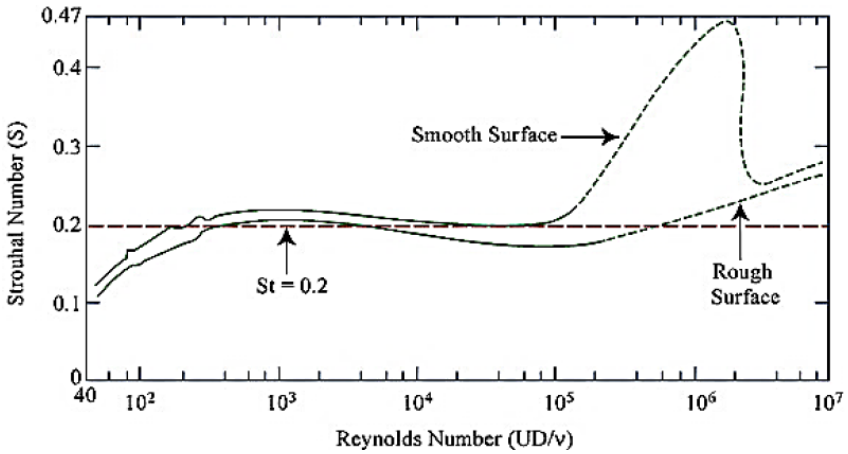

Fig. 7. Plot of Strouhal number *vs* Reynolds number

3.5 Pre-Processing

3.5.1 System domain

A CFD analysis requires high usage of computational resources. Therefore, only 2D representation of simulation (surface body) was chosen to conduct the analysis numerically. The system domain consists of an inlet (left), an outlet (right), a 2D cylinder (middle) and two walls (top and bottom).

There were several boundary conditions for the discretized equations. Some of them are inlet, outlet, wall and prescribed pressure [21].

The fluid flows from the inlet to outlet through subject study (cylinder) with walls as boundary conditions. Sufficient area of system domain was created to compromise between output results and computational time. The cylinder has a distance of 6D to the inlet, 15D to the outlet and 6D to both of side walls. The sketch of the system domain is shown in Figure 8.

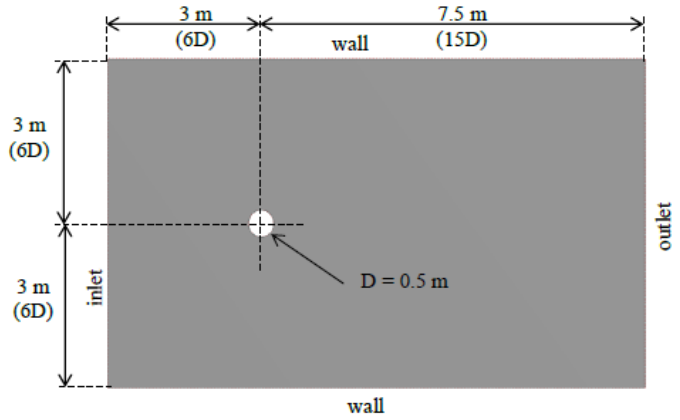

Fig. 8. System domain for analysis

3.5.2 Mesh generation

At the initial stage, the size of elements is set to be as coarse as possible, so that any solution glitch, due to geometry creation, during initial run could be detected earlier without contributing to time wastage. If there is no anomaly found, meshing with finer configurations is set up. There are in total of about 54 000 number of nodes and 75 000 number of elements used in the analysis. The elements consist of a mixture between quad and triad shape. Quad elements were concentrated at the critical area which is at the cylinder wall, while triad elements are located at the remaining locations. There are two mesh treatments applied in the creation of mesh. These are inflation and edge sizing. This is to ensure that the output results generated from the simulation are as accurate as possible, while compromising with the computational time taken to run a simulation. Details of the mesh configuration are shown in Table 4 and the mesh result is shown in Figure 9.

Table 4
Mesh details

Item	Parameters	Details
Statistical data	Number of nodes	54,085
	Number of elements	75,796
Mesh elements	Quad	At critical area (cylinder wall)
	Triad	Remaining location
Mesh treatment	Inflation	On cylinder wall
	Edge Sizing	On cylinder wall

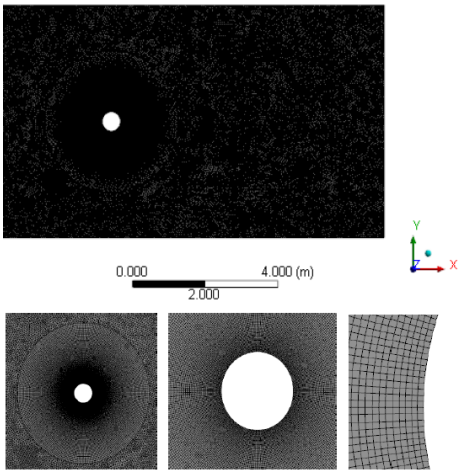

Fig. 9. Generated mesh in system domain (zooming in)

3.5.3 Time step

Timestep was derived from the Strouhal number for flow past a smooth cylinder. At least 20 to 25 timesteps was considered in one shedding cycle. Table 5 shows the details for setting up the time steps. Formula of Strouhal number is as Eq. (1),

$$St = \frac{f_s D}{U}. \quad (1)$$

Table 5
Mesh details

Load case no.	U m/s	Re -	St -	f Hz	t s	Time step min = t/25	taken
1	0.50	2.49E+05	0.27	0.27	3.70	0.15	0.100
2	1.00	4.98E+05	0.36	0.72	1.39	0.06	0.050
3	1.50	7.46E+05	0.40	1.20	0.83	0.03	0.025
4	2.00	9.95E+05	0.43	1.72	0.58	0.02	0.020

3.5.4 Solver execution

To numerically simulate the flow over cylinder problem, commercially available ANSYS Fluent 16 was utilized. The double-precision, pressure-based transient solver setup is summarized in Table 6.

Table 6
Fluent settings

Item	Remarks
Initialization	Hybrid
Reference value	Compute from inlet
Spatial discretization	Gradient: Least Square Cell Based Pressure: Second Order Momentum: Second Order Upwind
Transient formulation	Second Order Implicit
Convergence criteria	1×10^{-6} for continuity 1×10^{-6} for x and y velocity
Others	Max Iterations per Time step = 200

3.5.5 Assumptions and simplifications

To reduce complexity of numerical solution model, assumptions and simplifications are essential as long as it is able to represent the desired real or conceptual problem by retaining physically important features. For this study, list of all assumptions and simplifications are listed below.

- System domain adapted in the analysis is in 2D.
- No weathervane bearing was considered in the model.
- Fairing was always parallel to the dominant current flow direction.
- Fillet size of 0.05 m was designed at the fairing end. This also helped in producing good meshing.
- No change in temperature and fluid properties.

3.6 Post-processing

At this stage, graphs and contours for the output parameters such as drag coefficient (Cd), lift coefficient (Cl) and Strouhal (St) numbers were tabled and plotted to see the trends and patterns before conclusions could be made.

4. Results and Discussion

4.1 Data Comparison for Validation

The baseline model that was used throughout the different cylinder configurations, were determined based on the preliminary simulations performed in the Ansys Fluent software. After fine-tuning some miscellaneous parameters available in the software, two parameters such as the drag coefficient (Cd), as well as Strouhal number (St) were used for validation purpose and the results are shown in the following subsections.

4.1.1 Drag coefficient

The first validation for the baseline model was done using the comparison of the drag coefficient (Cd) between the results obtained from preliminary simulations and the established plot of drag coefficient (Cd) *vs* Reynolds number for a smooth cylinder. Figure 10 shows the results of drag coefficient when a bare cylinder was subjected to a flow with different speeds.

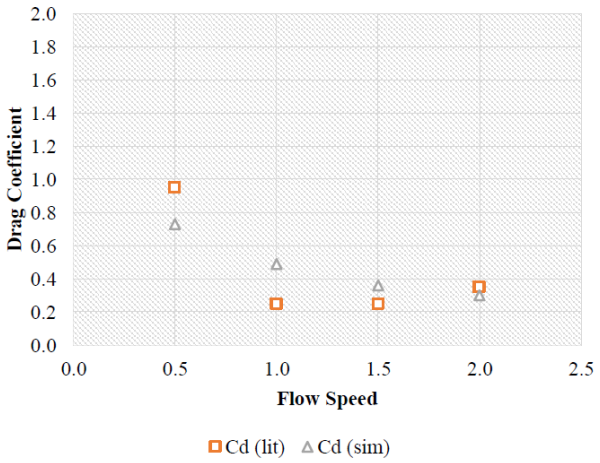

Fig. 10. Comparison of drag coefficient, Cd for bare cylinder with respect to flow speed

4.1.2 Strouhal Number

The second validation for the baseline model was done using the comparison of the Strouhal number (St) between the results obtained from preliminary simulations and the established plot of Strouhal number (St) *vs* Reynolds number for a smooth cylinder. Figure 11 shows the results for Strouhal Number when a bare cylinder was subjected to a flow with different speeds.

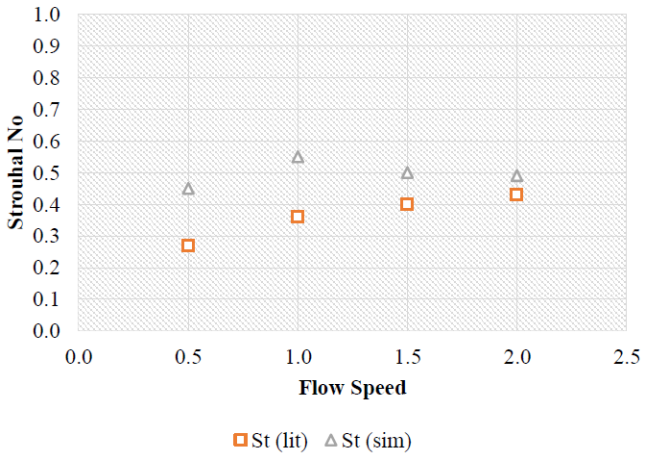

Fig. 11. Comparison of Strouhal number, St for bare cylinder with respect to flow speed

4.2 Results (Quantitative)

4.2.1 Results for set 1 (bare cylinder)

The comparison values for Strouhal and drag coefficient for bare cylinder at different flow speeds along with the respective lift coefficient and ratio of lift and drag coefficient are shown in Table 7. While the comparison values for Strouhal and drag coefficient for cylinder with fairing chord length of 1.25D and 1.5D at different flow speeds along with the respective lift coefficient and ratio of lift and drag coefficient are shown in Table 8 and 9 respectively.

Table 7
Results for set 1 (bare cylinder)

Load case no.	U m/s	Re -	St (lit) -	Cd (lit) -	St (sim) -	Cd (sim) -	Cl -	Cl/Cd ratio -
1	0.50	2.49E+05	0.27	0.95	0.45	0.73	0.79	1.08
2	1.00	4.98E+05	0.36	0.25	0.55	0.49	0.77	1.57
3	1.50	7.46E+05	0.40	0.25	0.50	0.36	0.51	1.42
4	2.00	9.95E+05	0.43	0.35	0.49	0.30	0.38	1.27

Table 8
Results for set 2 (fairing 1.25D)

Load case no.	U m/s	Re -	St -	Cd -	Cl -	Cd/Cl ratio -
1	0.50	2.49E+05	0.10	0.28	0.48	1.71
2	1.00	4.98E+05	0.23	0.17	0.27	1.59
3	1.50	7.46E+05	0.42	0.14	0.15	1.07
4	2.00	9.95E+05	0.40	0.18	0.19	1.06

Table 9
Results for set 3 (fairing 1. 5D)

Load case no.	U m/s	Re -	St -	Cd -	Cl -	Cd/Cl ratio -
1	0.50	2.49E+05	0.07	0.16	0.43	2.69
2	1.00	4.98E+05	0.02	0.12	0.41	3.42
3	1.50	7.46E+05	0.08	0.11	0.35	3.18
4	2.00	9.95E+05	0.20	0.08	0.21	2.63

4.3 Results (Qualitative)

A general comparison of qualitative result between the flow pattern for bare cylinder and cylinder with fairing of 1.25D chord length was made. Vortex shedding formation was relatively aggressive, faster and very close to the main structure for bare cylinder. This is shown in Figure 12. While for cylinder with fairing of 1.25D chord length, the vortex shedding formation was less aggressive, slower and further away from the main structure. This is shown in Figure 13.

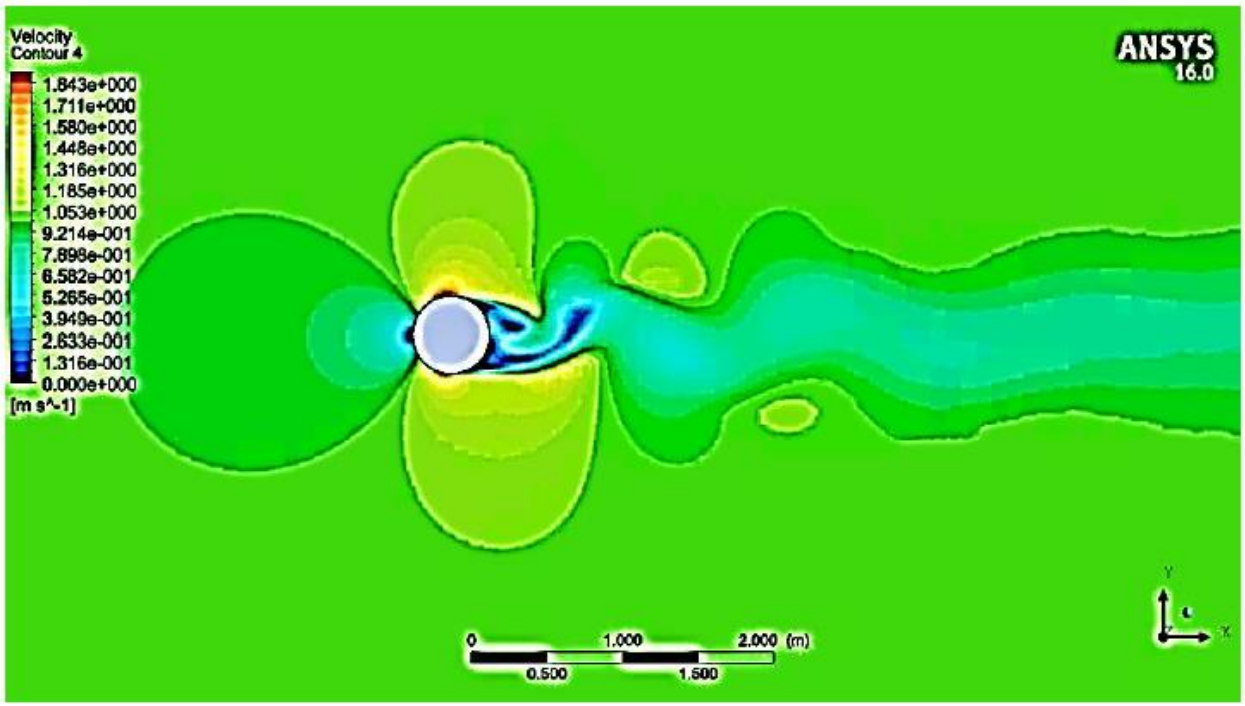

Fig. 12. Flow contour for bare cylinder subjected to flow speed of 1.0 m/s

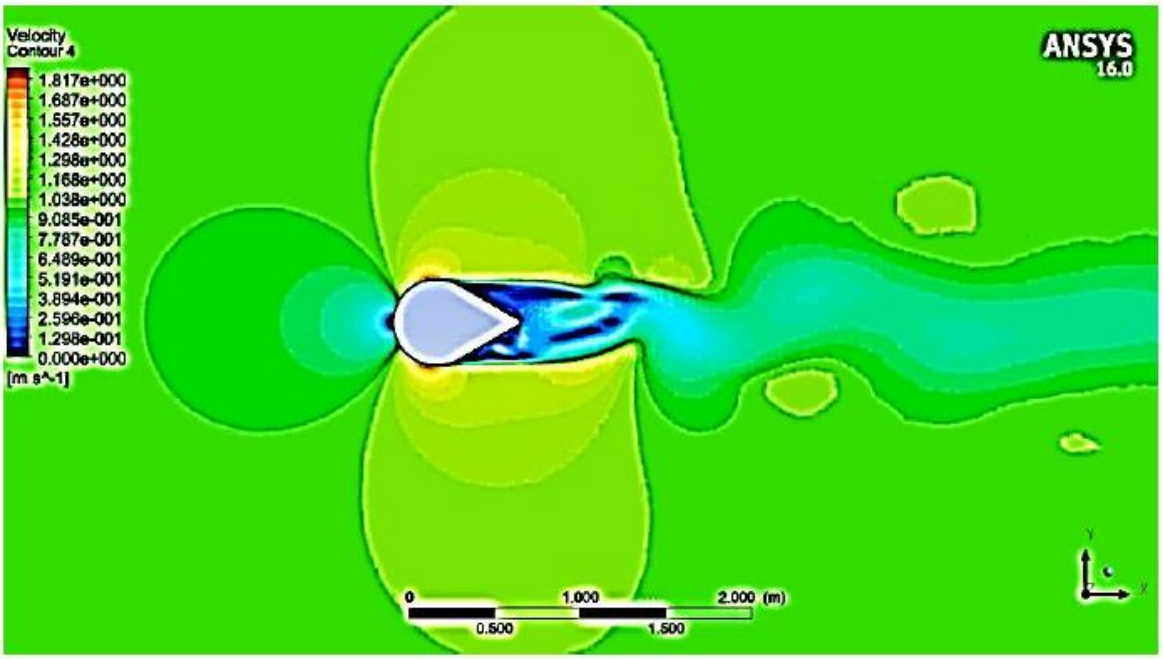

Fig. 13. Flow contour for cylinder with fairing 1.25D subjected to flow speed of 1.0 m/s

4.4 Results Based on Flow Speed

4.4.1 Analysis at flow speed of 0.5 m/s

The values for drag and lift coefficients for bare cylinder and cylinder with fairing of different chord lengths at flow speed of 0.5 m/s are shown in Table 10. The trends for drag and lift coefficients for bare cylinder and cylinder with fairing of different chord lengths at flow speed of 0.5 m/s are shown in Figure 14.

Table 10
Values of drag and lift coefficient at flow speed of 0.5 m/s for different cylinder conditions

Load case no.	Cylinder Type	Cd	Cl	Cd/Cl ratio
1	Bare	0.73	0.79	0.92
2	Fairing 1.25D	0.02	0.48	0.04
3	Fairing 1.5D	0.02	0.43	0.05

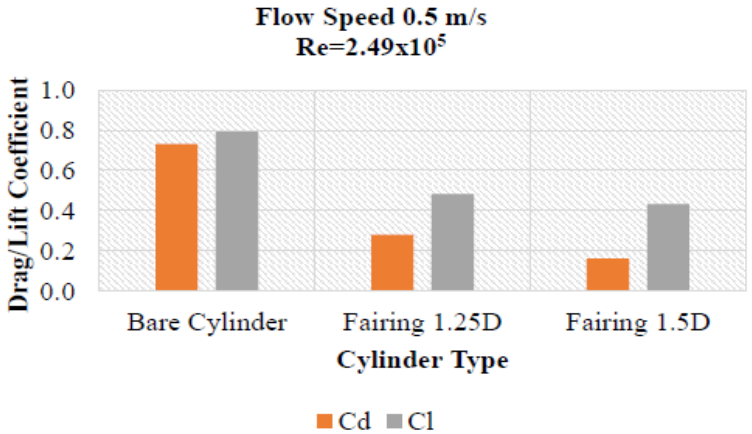

Fig. 14. Trend of drag and lift coefficient at flow speed of 0.5 m/s for different cylinder conditions

Drag coefficient reduces from bare cylinder to fairing with increasing chord length. Lift coefficient also reduces from bare cylinder to fairing with increasing chord length. Lift coefficient is more dominant than drag coefficient for all cylinder type. It would be possible that the cylinder with fairing length of 1.5D is at optimum condition for the flow speed of 0.5 m/s in the studied configurations.

4.4.2 Analysis at flow speed of 1.0 m/s

The values for drag and lift coefficients for bare cylinder and cylinder with fairing of different chord lengths at flow speed of 1.0 m/s are shown in Table 11. The trends for drag and lift coefficients for bare cylinder and cylinder with fairing of different chord lengths at flow speed of 1.0 m/s are shown in Figure 15. Drag coefficient reduces from bare cylinder to fairing with increasing chord length. Lift coefficient also reduced from bare cylinder to fairing with 1.25D chord length but increases back on fairing with 1.5D chord length. Lift coefficient was more dominant than drag coefficient for all cylinder types. It would be possible that the cylinder with fairing length of 1.25D was at optimum condition for the flow speed of 1.0 m/s in the studied configurations.

Table 11
Values of drag and lift coefficient at flow speed of 1.0 m/s for different cylinder conditions

Load case no.	Cylinder Type	Cd	Cl	Cd/Cl ratio
1	Bare	0.49	0.77	1.57
2	Fairing 1.25D	0.17	0.27	1.59
3	Fairing 1.5D	0.12	0.41	3.42

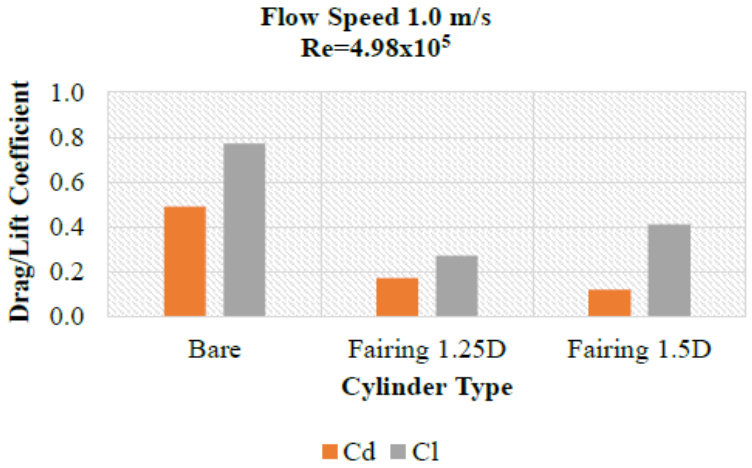

Fig. 15. Trend of drag and lift coefficient at flow speed of 1.0 m/s for different cylinder conditions

4.4.3 Analysis at flow speed of 1.5 m/s

The values for drag and lift coefficients for bare cylinder and cylinder with fairing of different chord lengths at flow speed of 1.5 m/s are shown in Table 12 and the trends for drag and lift coefficients for bare cylinder and cylinder with fairing of different chord lengths at flow speed of 1.5 m/s are shown in Figure 16. Drag coefficient reduces from bare cylinder to fairing with increasing chord length. Lift coefficient also reduces from bare cylinder to fairing with 1.25D chord length but increased back on fairing with 1.5D chord length. Lift coefficient was more dominant than drag coefficient for all cylinder types but fairing with 1.25D chord length has Cl/Cd ratio of almost 1 (equal

magnitude). It would be possible that the cylinder with fairing length of 1.25D is at optimum condition for the flow speed of 1.5 m/s in the studied configurations.

Table 12
Values of drag and lift coefficient at flow speed of 1.5 m/s for different cylinder conditions

Load case no.	Cylinder Type	Cd	Cl	Cd/Cl ratio
1	Bare	0.36	0.51	1.42
2	Fairing 1.25D	0.14	0.15	1.07
3	Fairing 1.5D	0.11	0.35	3.18

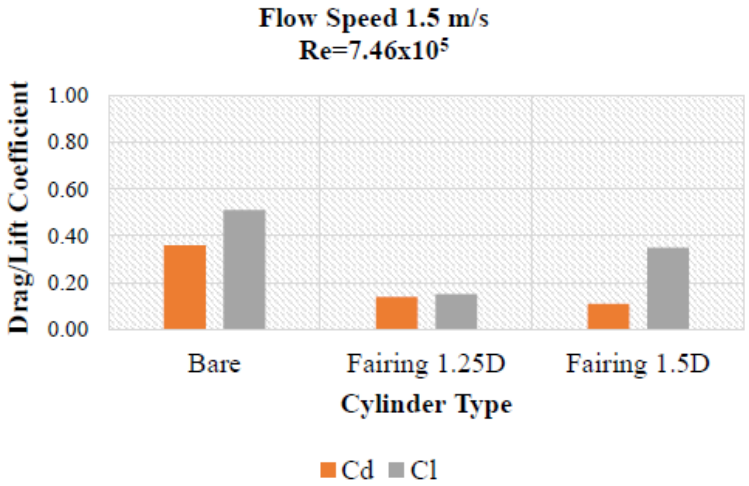

Fig. 16. Trend of drag and lift coefficient at flow speed of 1.5 m/s for different cylinder conditions

4.4.4 Analysis at flow speed of 2.0 m/s

The values for drag and lift coefficients for bare cylinder and cylinder with fairing of different chord lengths at flow speed of 2.0 m/s is shown are Table 13.

Table 13
Values of drag and lift coefficient at flow speed of 2.0 m/s for different cylinder conditions

Load case no.	Cylinder Type	Cd	Cl	Cd/Cl ratio
1	Bare	0.30	0.38	1.27
2	Fairing 1.25D	0.18	0.19	1.06
3	Fairing 1.5D	0.08	0.21	2.63

The trends for drag and lift coefficients for bare cylinder and cylinder with fairing of different chord lengths at flow speed of 2.0 m/s are shown in Figure 17. Drag coefficient reduces from bare cylinder to fairing with increasing chord length. Lift coefficient also reduces from bare cylinder to fairing with 1.25D chord length but increases back on fairing with 1.5D chord length. Lift coefficient was more dominant than drag coefficient for all cylinder type but fairing with 1.25D chord length has Cl/Cd ratio of almost 1 (equal magnitude). It would be possible that the cylinder with fairing length of 1.25D is at optimum condition for the flow speed of 2.0 m/s in the studied configurations.

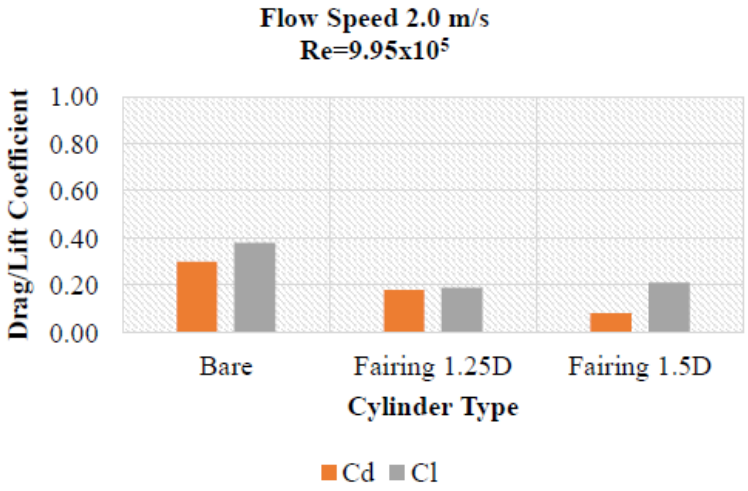

Fig. 17. Trend of drag and lift coefficient at flow speed of 2.0 m/s for different cylinder conditions

5. Conclusion

Flow around cylindrical structures is a classical subject, but still is interesting and relevant to investigate and study especially when the shape is changed to a more complex geometry. When a cylindrical structure such as a riser and conductor in oil and gas industry are subjected to continuous current flow, additional accessories such as faring can be applied on the structure to increase service life by reducing the drag as well as lift force, and hence reducing damage to the structure. This will be of great benefit to the platform operator in terms of reducing the maintenance cost.

It is found from this investigation that increasing the fairing chord length will reduce the drag coefficient (Cd) of the cylindrical structure, but not necessarily to reduce the lift coefficient further as the drag coefficient (Cd) getting higher. The lift coefficient (Cl) could be lowest at the optimum fairing chord length. Validation on numerical solution model shows that results for few parameters such as drag coefficient (Cd) and Strouhal number (St) was in good agreement with the data from the literature. Thus, reliability of the CFD solution method executed in this study is relatively solid and hence is referable for future studies.

CFD simulation study for VIV is still not fully matured due to limitations of computational resources. Very few researches have done on VIV effect for high Reynolds number. Furthermore, there is still no solid relationship between geometry of fairing with the amplitude of VIV has been established. Therefore, understanding on VIV is still being improved and better prediction of VIV phenomena is still being developed and explored.

The analysis of VIV suppression device using fairing performed here could be improved and extended further in future. It is recommended to run more simulations with different cylinder configurations. In other words, the fairing chord can be varied further to a length of 2D to 5D to see the effects of change in terms of drag coefficient and lift coefficient produced.

Another recommendation was to perform the simulation in 3D and enabling fluid structure interaction (FSI) of either 1 or 2 ways for better result agreement with experimental data. The analysis can also be solved using different turbulence models and comparison can be made to see the correlation with other analysis approach. Both approaches however require greater computational time and resources.

It is also recommended to run the analysis with different arrangement of cylinders should it be performed in 3D. The cylinder can be arranged in either vertical, horizontal or even in an angle position. To increase the variation of the study, the cylinder could also be set up in tandem

arrangement. All of the variations would produce a more complex correlation that would be useful to the industry when selecting the fairing configuration according to its applications.

Scale model experiment should be conducted in the laboratory to compare the agreements of results between the one performed in simulation and laboratory experiment. Should the cost of study be no longer become a limitation, actual experiment in open sea could be conducted. However, a lot of sensors need to be installed to measure the results obtained and intensive post processing was required to filter the unwanted noise from the data.

Finally, it is recommended to run the analysis with different types of VIV suppression device such as helical strake, rope, shroud and vane. Some of the devices mentioned here could perform better than others and the pros and cons could be studied to an extended detail.

References

[1] Blevins, Robert D. "Flow-induced vibration." *New York* (1977). https://doi.org/10.1115/1.3424205

[2] Nakamura, Tomomichi, Shigehiko Kaneko, Fumio Inada, Minoru Kato, Kunihiko Ishihara, Takashi Nishihara, Njuki W. Mureithi, and Mikael A. Langthjem, eds. *Flow-induced vibrations: classifications and lessons from practical experiences*. Butterworth-Heinemann, 2013.

[3] Gao, Yun, Shixiao Fu, Leixin Ma, and Yifan Chen. "Experimental investigation of the response performance of VIV on a flexible riser with helical strakes." *Ships and Offshore Structures* 11, no. 2 (2016): 113-128. https://doi.org/10.1080/17445302.2014.962788

[4] Morison, J. R., Joseph W. Johnson, and Samuel A. Schaaf. "The force exerted by surface waves on piles." *Journal of Petroleum Technology* 2, no. 05 (1950): 149-154. https://doi.org/10.2118/950149-G

[5] Rahman, Md Mahbubar, Md Mashud Karim, and Md Abdul Alim. "Numerical investigation of unsteady flow past a circular cylinder using 2-D finite volume method." *Journal of Naval Architecture and Marine Engineering* 4, no. 1 (2007): 27-42. https://doi.org/10.3329/jname.v4i1.914

[6] Patnana, Vijaya K., Ram P. Bharti, and Raj P. Chhabra. "Two-dimensional unsteady flow of power-law fluids over a cylinder." *Chemical Engineering Science* 64, no. 12 (2009): 2978-2999. https://doi.org/10.1016/j.ces.2009.03.029

[7] Mittal*, S., and V. Kumar. "Vortex induced vibrations of a pair of cylinders at Reynolds number 1000." *International Journal of computational fluid dynamics* 18, no. 7 (2004): 601-614. https://doi.org/10.1080/1061856031000137017

[8] Shao, J., and C. Zhang. "Large eddy simulations of the flow past two side-by-side circular cylinders." *International Journal of Computational Fluid Dynamics* 22, no. 6 (2008): 393-404. https://doi.org/10.1080/10618560802163838

[9] Bourguet, Rémi, George E. Karniadakis, and Michael S. Triantafyllou. "Lock-in of the vortex-induced vibrations of a long tensioned beam in shear flow." *Journal of Fluids and Structures* 27, no. 5-6 (2011): 838-847. https://doi.org/10.1016/j.jfluidstructs.2011.03.008

[10] Patil, Pratish P., and Shaligram Tiwari. "Numerical investigation of laminar unsteady wakes behind two inline square cylinders confined in a channel." *Engineering Applications of Computational Fluid Mechanics* 3, no. 3 (2009): 369-385. https://doi.org/10.1080/19942060.2009.11015277

[11] Mhalungekar, Chandrakant D., and P. Wadkar Swapnil. "CFD and Experimental analysis of vortex shedding behind D-shaped cylinder." *International Journal of Innovative Research in advanced engineering* (2014).

[12] Kianifar, Ali, and Edris Yousefi Rad. "Numerical simulation of unsteady flow with vortex shedding around circular cylinder." *momentum* 2 (2010): 1.

[13] Roshko, Anatol. "Experiments on the flow past a circular cylinder at very high Reynolds number." *Journal of fluid mechanics* 10, no. 3 (1961): 345-356. https://doi.org/10.1017/S0022112061000950

[14] Oliveira, Marcos André de, Paulo Guimarães de Moraes, Crystianne Lilian de Andrade, Alex Mendonça Bimbato, and Luiz Antonio Alcântara Pereira. "Control and suppression of vortex shedding from a slightly rough circular cylinder by a discrete vortex method." *Energies* 13, no. 17 (2020): 4481. https://doi.org/10.3390/en13174481

[15] Sunil, A. S., and PS TIDE. "An Investigation on flow oscillations due to shear layer instability and vortex dynamics." PhD diss., Cochin University of Science and Technology, 2020.

[16] Zhang, Hongfu, Lei Zhou, Tingting Liu, Zijian Guo, and Farshad Golnary. "Dynamic mode decomposition analysis of the two-dimensional flow past two transversely in-phase oscillating cylinders in a tandem arrangement." *Physics of Fluids* 34, no. 3 (2022). https://doi.org/10.1063/5.0079884

[17] Chen, Wen-Li, Yewei Huang, Changlong Chen, Haiyang Yu, and Donglai Gao. "Review of active control of circular cylinder flow." *Ocean Engineering* 258 (2022): 111840. https://doi.org/10.1016/j.oceaneng.2022.111840

[18] Alcântara Pereira, Luiz Antonio, Marcos André de Oliveira, Paulo Guimarães de Moraes, and Alex Mendonça Bimbato. "Numerical experiments of the flow around a bluff body with and without roughness model near a moving wall." *Journal of the Brazilian Society of Mechanical Sciences and Engineering* 42 (2020): 1-17. https://doi.org/10.1007/s40430-020-2217-6

[19] Rostami, Ali Bakhshandeh, Mohammad Mobasheramini, and Antonio Carlos Fernandes. "Strouhal number of flat and flapped plates at moderate Reynolds number and different angles of attack: experimental data." *Acta Mechanica* 230 (2019): 333-349. https://doi.org/10.1007/s00707-018-2292-2

[20] Park, Sehjin, Ho-Seong Sohn, Hyung Hee Cho, Hee Koo Moon, Yang Seok Han, and Osamu Ueda. "Effects of wakes on blade endwall heat transfer in high turbulence intensity." *Journal of Turbomachinery* 142, no. 2 (2020): 021002. https://doi.org/10.1115/1.4045335

[21] Versteeg, Henk Kaarle, and Weeratunge Malalasekera. *An introduction to computational fluid dynamics: the finite volume method*. Pearson education, 2007.